Retinal Cases and Brief Reports Publish Ahead of Print
DOI: 10.1097/ICB.0000000000001208

NPHP1 Full Deletion Causes Nephronophthisis and a Cone-Rod Dystrophy

Zujaja Tauqeer, M.D.[1], *Erin C. O'Neil, M.D.*[1,2], *Alexander J. Brucker, M.D.* [1], *Tomas S. Aleman, M.D.*[1,2]

[1]Scheie Eye Institute

[2]The Center for Advanced Retinal and Ocular Therapeutics, Department of Ophthalmology, University of Pennsylvania, Philadelphia, Pennsylvania

Funding: Supported by grants from Foundation Fighting Blindness, Hope for Vision, Macula Vision Research Foundation, the Paul and Evanina Bell Mackall Foundation Trust and The Pennsylvania Lions Sight Conservation and Research Foundation.

Declaration of Interest: No conflict of interest related to this work for any of the authors.

Corresponding author: Tomas S. Aleman, Perelman Center for Advanced Medicine, University of Pennsylvania, 3400 Civic Center Boulevard, Philadelphia, PA 19104. Tel: +1 215 662 8676; Fax: +1 215 615 0527, Email: aleman@pennmedicine.upenn.edu

Short title: *NPHP1*-associated cone-rod dystrophy

Precis

NPHP1-associated retinal degeneration can present as a cone-rod dystrophy with relative foveal preservation. This phenotype is increasingly recognized in other oculo-renal ciliopathies, such as Bardet-Biedl and Alstrom syndromes, suggesting common or intersecting mechanism of disease. This report also supports there may be a consistent *NPHP1*-retinal phenotype rather than diversity.

Abstract:

Purpose: To describe in detail the structural and functional phenotype of a patient with cone-rod dystrophy associated with a full deletion of the *NPHP1* gene.

Methods: A 30-year-old male with history of end-stage renal disease (ESRD) presented with progressive vision loss in early adulthood prompting evaluation for retinal disease. Ophthalmic evaluation was performed including, kinetic fields, electroretinography (ERG), spectral domain optical coherence tomography (SD-OCT), fundus auto-fluorescence (FAF), wide-angle fluorescein angiography and near infrared imaging (NIR).

Results: Visual acuity was 20/60 in each eye. Fundus examination revealed a subtle bull's-eye maculopathy confirmed with fundus autofluorescence. SD-OCT demonstrated perifoveal loss of the outer retinal layers with structural preservation further peripherally. Testing of retinal function confirmed loss of cone greater than rod sensitivities in a manner that co-localized to structural findings. ERG revealed decreased photopic and scotopic responses. Genetic testing confirmed a homozygous whole gene deletion of the *NPHP1* gene.

Conclusion: *NPHP1*-associated retinal degeneration may present as a cone-rod dystrophy in addition to the previously reported rod-predominant phenotypes and can notably be associated with systemic abnormalities, including renal disease. Our work further expands upon the growing literature describing retinal disease associated with systemic ciliopathies.

Key words: *NPHP1, Senior-Loken syndrome, ciliopathies, fundus autofluorescence cone-rod dystrophy, OCT*

INTRODUCTION

Inherited retinal degenerations (IRDs) may be associated with a number of systemic findings including neurologic, cardiac, renal, and hearing abnormalities.[1] Patients may present to the eye clinic with isolated visual symptoms with a history of other organ dysfunction since childhood, or with an established systemic diagnosis that triggers the search for known associated ocular findings. Among retinal diseases with systemic associations, co-occurrence of retinal degenerations with renal diseases is well-known, as exemplified by Bardet-Biedl, Senior-Løken, Joubert, Jeune, Alström, and Meckel-Gruber syndromes.[2-8] The eponyms describe a molecularly heterogenous group of genetic conditions with variable severity of often overlapping phenotypic features.

Nephronophthisis (NPHP), the associated renal disease in these syndromes, comprises a genetically heterogeneous autosomal recessive group of diseases with a typical presentation in

childhood with fatigue and inability to concentrate urine causing polyuria and polydipsia, with ultrasound and histological evidence of cystic kidney changes.[9] The disease arises from dysfunction of the primary cilia in renal epithelial cells, caused by defects in genes that are essential for the normal development, maintenance, and function of the primary cilia.[10] The disease accounts for a significant proportion of end-stage renal disease, particularly in children and adolescents, although adult-onset renal disease has been reported.[3, 11] NPHP is caused by mutations in one of 13 *NPHP* genes, with 9 of these recognized to affect the retina. The largest proportion of NPHP cases is caused by mutations in *NPHP1* on 2q13 (OMIM 607100), a gene that encodes nephrocystin-1, an evolutionarily conserved, ubiquitously expressed protein that localizes to the transition zone of primary cilia and affects cells throughout the body ranging from the hair cells of the middle ear, to renal epithelial cells to the connecting cilium of photoreceptors; nephrocystin-1 is linked to other NPHP proteins through macromolecular complexes.[9, 12-14] In photoreceptors, nephrocystin-1 plays a critical role in intraflagellar transport.[9, 15, 16] Extra-renal manifestations are less frequent in *NPHP1*-associated nephronophthisis than in other *NPHP* gene-associated diseases. *NPHP1*-associated renal disease includes retinal abnormalities or vision loss in about 10-23% of the patients, depending on the source; other associations include Joubert syndrome, liver fibrosis (8%), and congenital oculomotor apraxia.[17-19]

There is paucity of descriptions of the retinal phenotype associated with *NPHP1* mutations, which contrasts with the wealth of descriptions of the associated renal disease. Reported phenotypes include early-onset and severe retinal degenerations associated with Senior-Loken syndrome, with pigmentary retinopathies classified as retinitis classic pigmentosa (RP) or patterns interpreted as ‘sectoral’ RP, nystagmus and severe vision loss in infancy

characteristic of Leber congenital amaurosis (LCA), as well as milder manifestations with central abnormalities and cone dysfunction classified as forms of cone-rod dystrophy.[2, 4, 9, 20-24]

In this report, we characterize in detail the retinal phenotype of a patient with a full deletion of *NPHP1* who presented with a history of end-stage renal disease and visual symptoms since early adulthood.[14] Through characterizing in detail the structural and functional phenotype of our patient, we hope to increase understanding of the pathophysiology of *NPHP1*-associated retinal disease as well as of related ciliopathies—diseases arising from mutated proteins in primary cilia—with retinal and renal involvement, including Senior-Loken and Bardet-Biedl syndromes.

METHODS

This is a retrospective review of the clinical record of a patient seen as part of standard of care. The visit adhered to HIPAA regulations and all personal identifiers have been removed. The patient underwent a complete ophthalmic examination, Goldmann kinetic fields, and Farnsworth D-15 color vision testing. Wide angle (200°) fundus imaging was performed using a scanning laser system (Optos Inc. Marlborough, MA). Spectral-domain optical coherence tomography (SD-OCT) and fundus autofluorescence (FAF) imaging using near infrared (NIR, 786 nm) and short wavelength (SW, 488 nm) excitation lights (emission: NIR = 810-900 nm; SW through barrier filter = 500-680 nm) were performed using a Spectralis-HRA system (Heidelberg Engineering GmbH, Heidelberg, Germany). Segmentation of the SD-OCT was performed with ImageJ analysis software [available in the public domain at https://imagej.nih.gov/ij/download.html]. Achromatic and chromatic (500 nm and 650 nm) static perimetry were performed using a modified Humphrey Field Analyzer (Carl Zeiss Meditec, Dublin, CA), following published methodology.[7] Thresholds were measured along the horizontal

meridian at 2˚ intervals, extending to 30˚ of eccentricity, corresponding to the retinal region scanned with SD-OCT as detailed above. Standard full-field electroretinograms (ERGs) were recorded using a computer-based system (Espion, Diagnosys LLC, Littleton, MA). Dark-adapted rod-mediated responses ('DA 0.01 protocol) were elicited with a dim white flash (0.01 cd.s.m^2); dark-adapted mixed cone-rod responses ('DA 3.0) were elicited with a standard flash (3.0 cd.s.m^2); light-adapted cone-mediated responses were elicited with the same stimulus in response to 1 Hz stimulation or a 30 Hz flicker.[7]

RESULTS

A 30-year-old male of Egyptian descent presented with slowly progressive decline in central vision in both eyes, with onset beginning around 20 years of age. He had been fitted with glasses around age 11. He was told at a young age that glasses 'would not help his vision' but was not formally diagnosed with a retinal disease, and thereafter had limited follow-up with eye care providers due to ongoing treatment for his complex underlying medical conditions. He was formally examined in his early 20s for difficulties seeing in daytime and in brightly illuminated places and a diagnosis of a cone dystrophy was entertained. Notably, he completed undergraduate education without major visual limitations.

His medical history was notable for onset of end-stage renal disease (ESRD) at age 11, the etiology of which was never uncovered, but variably attributed to "glomerulonephritis" and "autoimmune kidney disease" later in life while he was being monitored for dialysis and evaluated for kidney transplantation. The course of his renal disease was complicated by two failed renal transplants - a living donor kidney transplant from his father at age 12, which was explanted due to graft failure 2 months later, and a deceased donor kidney transplant as an adult, explanted in the immediate post-operative period due to a pseudoaneurysm of the external iliac-

renal artery anastomosis. He underwent nephrectomy of one native kidney as an adult for renal cell carcinoma, uncovered during surveillance testing while receiving treatment for Hepatitis C. Renal pathology demonstrated findings consistent with acquired cystic disease. In the interim, he remained stable on dialysis, however, the underlying etiology of his juvenile-onset ESRD remained undiagnosed. His review of systems was negative for deafness, polydactyly, abnormal cognition, seizures, ataxia or dysarthria, heart disease or arrhythmias, abnormal dentition or dysmorphic facies, abnormal bruising or bleeding or frequent infections, or gastrointestinal issues. Family history was notable for parental consanguinity (maternal and paternal grandfathers were brothers); there were no known relatives with visual complaints or renal problems (see pedigree, Supplemental Figure 1, http://links.lww.com/ICB/A150). Family members were not available for formal renal or ophthalmologic exams.

On exam, best corrected visual acuity was 20/60 in each eye (spherical equivalent = 0.50 D in each eye). Anterior segment examination was unremarkable. Extraocular motility was full. Fundus examination showed healthy appearing optic nerves and vessels in both eyes. There was a grayish appearance of the retinal pigment epithelium in the pericentral and near-midperipheral retina, most obvious in the temporal and nasal retina (Fig. 1A, *white arrows*). Wide-angle, short wavelength fundus autofluorescence (SW-FAF) showed hyperautofluorescence in the parafovea and along an oval band at the eccentricity of the vascular arcades (Fig. 1A, right panel). Just nasal to the nerve there was also an area of hypoautofluorescence (Fig. 1A, *short white arrow*). For comparison, conventional normal SW-FAF images are provided which are centered by a small (~2° diameter) dark region at the foveal center which is the result of absorption of the SW illumination by macular pigment (Fig. 1B, *left panel, inset*). An annular region (extending to ~5° from the fovea) of relatively low AF intensity surrounds this dark center, which is in turn

surrounded by the highest SW-AF intensities 10°-15° eccentric from the foveal center, which corresponds with the area of highest retinal pigment epithelium (RPE) lipofuscin content.[25] Closer inspection of the central SW-FAF images from the patient revealed the two bands of SW-hyperautofluorescence separated by normally appearing pericentral retina (Fig. 1B, *left panel, yellow arrows*). Normal NIR-FAF imaging is shown to demonstrate the expected appearance of a broad (~10° diameter) region of higher intensity signal that surrounds a maximum at the foveal center caused by higher RPE melanin content at that location (Fig.1B, *right panel, inset*).[25] In this patient's case, the parafoveal annulus was hyperautofluorescent on both NIR-FAF imaging (Fig. 1B) and SW-FAF imaging, as discussed previously. On NIR-FAF, a hypoautofluorescent foveal center is surrounded by the hyperfluorescent parafoveal annulus, which is in turn surrounded by a dense pericentral region of hypoautofluorescence that is delimited temporally from normal appearing midperipheral retina by a thin hyperautofluorescent line (Fig.1B, *right panel*).

A 9 mm-long horizontal SD-OCT cross-section from the fovea into temporal retina demonstrates a thin foveal center (98 µm; normal ± 2SD = 225 ± 28 µm) (Fig.1C). The outer nuclear layer (ONL) is detectable across the entire scan but is thinner than normal at the fovea (45 µm; normal ± 2SD = 106 ± 17 µm), and is nearly undetectable in the pericentral retina, but shows a gradual return to normal thickness (34 µm; normal ± 2SD = 46 ± 15 µm) at ~6 mm from the foveal center. A faint interdigitation signal (IZ) is only detectable at greater distance from the center, suggesting loss of the photoreceptor outer segments (POS) and photoreceptors in the central retina (Fig. 1C). The inner segment ellipsoid region band (EZ) is detectable at the foveola and in the pericentral and peripheral regions (Fig 1C). The hyperautofluorescent parafoveal annulus seen on SW-FAF and NIR-FAF corresponds to the transition in ONL thickness and loss

of the EZ signal in the parafovea (Fig. 1C, *white arrows*). The peripheral transition to better lamination and thickness at the temporal retina coincides with the hyperautofluorescent linear boundary in the NIR-FAF image (Fig. 1B,C, *long yellow arrow*).

Color vision measured with a Farnsworth-Munsell D15 test showed multiple major errors with a tritan axis of confusion in the right eye, without a defined axis in the left eye (Fig. 2A). Goldmann kinetic visual fields measured with a V-4e stimuli were full in peripheral extent with a pericentral absolute scotoma that spared fixation in both eyes; visual fields were limited to small inferior midperipheral islands when measured with the smallest (I-4e) target (Fig. 2B). A full-field electroretinogram (ffERG) showed abnormally reduced amplitudes for both rod and cone-mediated responses with proportionally greater loss of cone mediated function (Fig. 2C). Rod ERGs elicited with a dim white flash were reduced to 25% of the normal b-wave amplitudes (60 µV; normal ± 2SD = 250 ± 143 µV), whereas cone ERGs in response to a 30Hz flicker showed greater reductions in amplitude at only 16% of normal (17 µV; normal = 107 ±33 µV) (Fig 2C). Rod- and cone-mediated function was also measured with chromatic static perimetry (dark-adapted with 500 nm and 650 nm; light-adapted achromatic stimulus) (Fig. 2D). Mediation by rod or cone photoreceptors was determined by comparing dark-adapted sensitivities to the 500 nm and 650 nm stimuli. Sensitivities were measured at 2° intervals along the horizontal meridian co-localizing with the regions scanned with SD-OCT. Sensitivity profiles revealed a central island of severely reduced cone-mediated function (by at least a log unit) separated from a nasal field island of near-normal rod vision with abnormal cone function (Fig. 2B).

The patient's retinal dysfunction in association with his systemic disease raised suspicion for a syndromic IRD. Targeted gene sequencing (GeneDx, Retinal Dystrophy Xpanded Test, 770 genes, Gaithersburg, Maryland, USA) detected a homozygous deletion of the entire *NPHP1* gene

on locus 2q13, as has been reported in association with NPHP.[14] Other variants detected consisted of a missense variation in exon 8 of the VCAN gene (p.Thr1889lle (ACA > ATA): c.5666 C>T); i*n silico* gene analysis predicted no alteration of protein structure or function. There were no other homozygous combinations of genes known to cause recessively inherited retinal degenerations. MRI imaging of the brain was undertaken and revealed mild atrophy of the superior cerebellum without the 'molar tooth sign' cerebellar vermis abnormality that is characteristic of Joubert Syndrome (Supplemental Figure 2, http://links.lww.com/ICB/A151).[8]

DISCUSSION

Reports to date of the retinal phenotype associated with NPHP1 are mostly limited to denoting the general phenotypic category the patients may be belong to, likely due to the considerably greater focus on the renal disease, which is well-known in the literature and is the most common genetic cause of end-stage renal disease in childhood and early adulthood. The descriptions of the associated retinal disease range from early and severe photoreceptor degenerations as classically described in Senior-Løken syndrome, to pigmentary retinopathies that may be classified as belonging to the umbrella diagnostic group of RP, and even instances where the retinal disease may be subtle or relatively asymptomatic.[2, 4, 5, 9, 20-24] An important question is whether the retinal phenotypes represent phenotypic diversity, or a common phenotype modulated by disease severity, and thus dependent on the window in time within the natural history of the disease when diagnosis is made. The patient reported herein presented with hemeralopia or poor central vision in photopic conditions in early adulthood, but may have been symptomatic from earlier in life. Multimodal imaging showed a severe central to near midperipheral photoreceptor degeneration with a relatively spared fovea, which supported sufficient foveal vision that allowed the patient to cope with his visual symptoms and function

independently well into the fourth decade of life. Slightly greater cone relative to rod photoreceptor dysfunction was confirmed by full-field ERGs, and locally severe pericentral rod and cone dysfunction determined by dark-adapted perimetry correlated with severe photoreceptor loss on SD-OCT. This phenotype is consistent with subtypes of cone-rod dystrophies, including a report of *NPHP1*-associated IRD, explains pauci-symptomatic *NPHP1*-associated retinal disease as foveal vision may be supported by relative spared foveal centers, and closely resembles the regional pattern of disease recently documented in two *NPHP1*-associated IRD cases interpreted as Senior-Løken syndrome associated with 'sectoral RP'.[20, 21, 26, 27] Our findings suggest there may be indeed phenotypic consistency in *NPHP1*-associated disease as a CRD or predominantly central photoreceptor degeneration modulated by disease severity into apparently dissimilar phenotypes.

NPHP1-associated retinal degeneration may be added to the list of ciliopathies—diseases arising from genetic defects in proteins of the primary cilia—that have systemic manifestations and show a predominantly central to near midperipheral disease and/or a CRD pattern of dysfunction. The list includes Alström, *INPP5E*-associated retinopathies (isolated or as part of Joubert syndrome), Jalili, Lawrence-Moon, and Bardet Biedl syndromes (Supplemental Tables, http://links.lww.com/ICB/A149).[7] Underrepresentation of the central to near midperipheral photoreceptor degeneration pattern in the *NPHP1* literature may either represent true phenotypic diversity, or be due to extension of a predominant central disease into a retina-wide degeneration. By the time the disease presents symptomatically, an earlier cone>rod phenotype may have converged into a severe, retina-wide rod and cone photoreceptor degeneration associated with a pigmentary retinopathy indistinguishable from 'RP'. This 'morphing' sequence may be better recognized with earlier molecular diagnoses and characterization of minimally symptomatic

(visually) individuals in the setting of *NPHP1*-associated ('isolated') renal disease using multimodal structural and functional testing.[20, 28] It may be informative to use specialized testing, such as full-field psychophysics, to ask if the severe retina-wide disease previously reported with *NPHP1*-LCA/Senior-Løken syndrome may represent the severe end of the spectrum of the phenotype described herein.

Whereas intraretinal variation in disease severity is common in IRD, it is unclear why should there be such a predilection for central manifestations in certain subtypes, as exemplified in our patient. Multimodal imaging showed an oval region of central abnormalities extending along the horizontal axis, beyond the eccentricity of the optic nerve. NIR-FAF showed a heavily demelanized hypoautofluorescent pericentral retina that was not obvious on fundus exam, and which contrasted with a hyperautofluorescent pattern on SW-FAF within the same region. The inner (toward the foveal center) and outer boundaries of this region corresponded to a transition from severely thinned ONL with shorten or absent outer segments (undetectable EZ and/or IZ) to a more normal appearance on the OCT cross-sections, from abnormal to normal fundus autofluorescent patterns for both excitation lights, and from severely depressed cone>rod sensitivities to better vision on co-localized, two-color, dark-adapted sensitivity profiles. This horizontal asymmetry is reminiscent of the nasally displaced cone densities described by histology where cone densities extend more along the horizontal meridian, particularly toward the nasal retina.[29] The topography has been described in molecularly diverse forms of IRDs with a central predilection, in two *NPHP1*-associated cases interpreted as sector RP, as well as in *CNNM4*-associated Jalili syndrome, a genetic disease mechanistically linked to *IQCB1*/*NPHP5*, a gene that when mutated is invariably associated with Senior-Løken syndrome (Supplemental Tables).[2, 21]

The FAF topography suggests that the loss of cone and rod photoreceptor within this region may lead to, or be associated with, the loss of the melanin signal originating from otherwise detectable RPE cells that still contain lipofuscin, the main fluorophore underlying the SW-FAF signal.[25] It is also possible that the central apparent hyperautofluorescence on SW-FAF may originate from reduced 'screening' of the incoming SW excitation light by shortened or absent photoreceptor outer segments with resultant greater transmission of RPE lipofuscin autofluorescence, in addition to overload of the RPE cell by shed outer segments as the result of the photoreceptor degeneration. This dissociation between NIR- and SW-FAF has been documented in a number of retinopathies with a significant or primary involvement of the RPE in their pathophysiology.[30] The pattern of RPE demelanization in *NPHP1*-IRD may reflect a failure of the mutual interdependence of photoreceptors and RPE cells in this region of higher combined rod and cone photoreceptor densities.[7, 29]

Senior-Løken syndrome describes an autosomal recessive association of NPHP and a childhood-onset retinal degeneration, within the spectrum of Leber Congenital Amaurosis.[4, 5] In the literature, however, the syndrome has become synonymous to the association between NPHP and IRDs in the absence of other systemic abnormalities. The patient in this report is an example, as the retinal manifestations does not match the original description of Senior-Løken syndrome. In this era of precise molecular diagnoses, it may be more accurate to denote the disease as an *NPHP1*-associated oculo-renal syndrome, part of a genetically heterogenous disorders with various eponyms. The underlying commonality between retinal and renal abnormalities in most of the molecular causes within this group of conditions is an abnormality at the primary cilia, such as disrupted protein trafficking and abnormal formation, maintenance, and function of the photoreceptors outer segment and the cilia of renal tubular cells. Nephrocystin-1 localizes to the

connecting cilium in close proximity to the basal bodies, curiously, where BBS proteins co-localize.[12, 16] This is notable as *BBS* mutations cause Bardet-Biedl syndrome, probably the best known of the oculo-renal syndromes with potentially common mechanisms.[16] The failure in protein compartmentalization within the photoreceptor inner and outer segment presumably triggers apoptotic signals that ultimately cause a retina-wide photoreceptor degeneration.[16] Molecular investigations have not, for the most part, elucidated how a ciliopathy may contribute to a rod versus cone predominant disease or why should there be involvement of the central retina. The sources of the pattern of functional and structural abnormalities in *NHPH1*-Senior-Løken syndrome and in a number of clinically and/or molecularly related conditions certainly deserves further exploration as they may be the key to unveil common mechanisms and hopefully treatments for both the renal as well as the retinal disease.

REFERENCES

1. Werdich XQ, Place EM, Pierce EA. Systemic Diseases Associated with Retinal Dystrophies. *Seminars in Ophthalmology* 2014;29:319-328.

2. Ronquillo CC, Bernstein PS, Baehr W. Senior-Loken syndrome: a syndromic form of retinal dystrophy associated with nephronophthisis. *Vision Res* 2012;75:88-97.

3. Savige J, Ratnaike S, Colville D. Retinal abnormalities characteristic of inherited renal disease. *J Am Soc Nephrol* 2011;22:1403-1415.

4. Loken AC, Hanssen O, Halvorsen S, Jolster NJ. Hereditary renal dysplasia and blindness. *Acta Paediatr* 1961;50:177-184.

5. Senior B, Friedmann AI, Braudo JL. Juvenile familial nephropathy with tapetoretinal degeneration. A new oculorenal dystrophy. *Am J Ophthalmol* 1961;52:625-633.

6. Devlin LA, Sayer JA. Renal ciliopathies. *Current Opinion in Genetics & Development* 2019;56:49-60.

7. Aleman TS, O'Neil EC, O'Connor K, et al. Bardet-Biedl syndrome-7 (BBS7) shows treatment potential and a cone-rod dystrophy phenotype that recapitulates the non-human primate model. *Ophthalmic Genet* 2021;1-14.

8. Tory K, Lacoste T, Burglen L, et al. High NPHP1 and NPHP6 Mutation Rate in Patients with Joubert Syndrome and Nephronophthisis: Potential Epistatic Effect of NPHP6 and AHI1 Mutations in Patients with NPHP1 Mutations. *Journal of the American Society of Nephrology* 2007;18:1566-1575.

9. Hildebrandt F, Attanasio M, Otto E. Nephronophthisis: Disease Mechanisms of a Ciliopathy. *Journal of the American Society of Nephrology* 2009;20:23-35.

10. Youn YH, Han Y-G. Primary Cilia in Brain Development and Diseases. *The American Journal of Pathology* 2018;188:11-22.

11. Snoek R, Van Setten J, Keating BJ, et al. NPHP1 (Nephrocystin-1) Gene Deletions Cause Adult-Onset ESRD. *Journal of the American Society of Nephrology* 2018;29:1772-1779.

12. Fliegauf M, Horvath J, Von Schnakenburg C, et al. Nephrocystin Specifically Localizes to the Transition Zone of Renal and Respiratory Cilia and Photoreceptor Connecting Cilia. *Journal of the American Society of Nephrology* 2006;17:2424-2433.

13. Antignac C, Arduy CH, Beckmann JS, et al. A gene for familial juvenile nephronophthisis (recessive medullary cystic kidney disease) maps to chromosome 2p. *Nat Genet* 1993;3:342-345.

14. Konrad M, Saunier S, Heidet L, et al. Large homozygous deletions of the 2q13 region are a major cause of juvenile nephronophthisis. *Hum Mol Genet* 1996;5:367-371.

15. Jiang ST, Chiou YY, Wang E, et al. Essential role of nephrocystin in photoreceptor intraflagellar transport in mouse. *Hum Mol Genet* 2009;18:1566-1577.

16. Datta P, Cribbs JT, Seo S. Differential requirement of NPHP1 for compartmentalized protein localization during photoreceptor outer segment development and maintenance. *PLOS ONE* 2021;16:e0246358.

17. Konig J, Kranz B, Konig S, et al. Phenotypic Spectrum of Children with Nephronophthisis and Related Ciliopathies. *Clin J Am Soc Nephrol* 2017;12:1974-1983.

18. Tang X, Liu C, Liu X, et al. Phenotype and genotype spectra of a Chinese cohort with nephronophthisis-related ciliopathy. *Journal of Medical Genetics* 2020;jmedgenet-2020-.

19. Chaki M, Hoefele J, Allen SJ, et al. Genotype–phenotype correlation in 440 patients with NPHP-related ciliopathies. *Kidney International* 2011;80:1239-1245.

20. Caridi G, Murer L, Bellantuono R, et al. Renal-retinal syndromes: association of retinal anomalies and recessive nephronophthisis in patients with homozygous deletion of the NPH1 locus. *Am J Kidney Dis* 1998;32:1059-1062.

21. Yahalom C, Volovelsky O, Macarov M, et al. Senior- Loken Syndrome: A Case Series and Review of The Reno-Retinal Phenotype and Advances of Molecular Diagnosis. *Retina* 2021.

22. Bollée G, Fakhouri F, Karras A, et al. Nephronophthisis related to homozygous NPHP1 gene deletion as a cause of chronic renal failure in adults. *Nephrology Dialysis Transplantation* 2006;21:2660-2663.

23. Godel V, Luna A, Nemet P, Lazar M. Retinal manifestations in familial juvenile nephronophthisis. *Clinical Genetics* 2008;16:277-281.

24. Ning K, Song E, Sendayen BE, et al. Defective INPP5E distribution in NPHP1-related Senior–Loken syndrome. *Molecular Genetics & Genomic Medicine* 2021;9.

25. Keilhauer CN, Delori FC. Near-infrared autofluorescence imaging of the fundus: visualization of ocular melanin. *Invest Ophthalmol Vis Sci* 2006;47:3556-3564.

26. Szlyk JP, Fishman GA, Alexander KR, Peachey NS, Derlacki DJ. Clinical subtypes of cone-rod dystrophy. *Arch Ophthalmol* 1993;111:781-788.

27. Birtel J, Eisenberger T, Gliem M, et al. Clinical and genetic characteristics of 251 consecutive patients with macular and cone/cone-rod dystrophy. *Sci Rep* 2018;8:4824.

28. Matsui R, McGuigan Iii DB, Gruzensky ML, et al. SPATA7: Evolving phenotype from cone-rod dystrophy to retinitis pigmentosa. *Ophthalmic genetics* 2016;37:333-338.

29. Curcio CA, Sloan KR, Packer O, Hendrickson AE, Kalina RE. Distribution of cones in human and monkey retina: individual variability and radial asymmetry. *Science* 1987;236:579-582.

30. O'Neil E, Uyhazi, KE, Connor, KO, Aleman, IA, Pulido, JS, Rossano, JW, Aleman, TS. Danon Disease: A model of photoreceptor degeneration secondary to primary retinal pigment epithelium disease. . *Retina Cases and Brief Reports 2021* 2021.

FIGURE LEGENDS

FIGURE 1. En-face multimodal and cross-sectional imaging in a patient with a full deletion of *NPHP1*. **A.** Wide angle color fundus photography and fundus autofluorescence elicited with short-wavelength (SW-FAF) excitation light. White square delimits a 30° field, green line is the position of the SD-OCT scan, described in B and C, respectively. **B.** Central (30°) SW- and near-infrared (NIR) fundus autofluorescence (FAF) imaging in the patient. Normal SW-FAF and NIR-FAF images are shown as insets. Arrows of different length delimit hyper-autofluorescent

regions (short = central limit, long arrow = peripheral limit) in the parafovea (*white arrows*) and pericentral (*yellow arrows*) retina. **C.** SD-OCT horizontal, 9 mm cross sections through the fovea and into the temporal retina in the patient. The location of the scan is denoted with a green arrow in (A). A magnified section from the temporal retina in a normal subject is shown as an inset for comparison. Nuclear layers are labeled: outer nuclear layer = ONL, inner nuclear layer = INL, ganglion cell layer = GCL. Outer retinal sublaminae are labelled (*diagonal arrows*) according to conventional nomenclature: 1. Outer limiting membrane (OLM), 2. Inner segment ellipsoid region (ISe or EZ), 3. The contact cylinder between the apical RPE microvilli and the photoreceptor outer segments tips, or interdigitation zone (IZ), 4. Basal RPE and Bruch's membrane (RPE/BrM). Vertical yellow arrows in the patients denote juxtafoveal segment with abrupt outer retinal (OLM, EZ and IZ) and FAF changes. *White arrows* a denote segment between the point where the EZ (*short arrow*) and OLM (*long arrow*) become undiscernible that corresponds to a hyper-autofluorescent parafoveal halo on SW- and NIR-FAF imaging in (B). The long *yellow arrow* points to a location ~6 mm from the foveal center where the retina transitions from retina with a thinned ONL and absent EZ to a near-normal appearance that corresponds to the thin peripheral hyper-autofluorescent line on NIR-FAF in (B). The pericentral retina with thinned ONL and non-discernible EZ and IZ between the two long arrows corresponds to the region with either normal or increased (more peripherally) SW-FAF, but deeply depigmented hypo-autofluorescent retina on NIR-FAF in (B). Scale bar to the left. T, temporal.

FIGURE 2. Visual function in a patient with a full deletion of *NPHP1*. **A.** Color vision measured with a Farnsworth-Munsell D15 test. Lines connect the order of the caps as ordered by

the patient. The normal result is a circle with a left slit (between cap 15 and the reference cap). **B.** Kinetic visual fields in the patient. Right eye on (A) and (B) is displayed on the right per convention. **C.** Standard full-field ERGs in the patient compared with a representative normal subject (gray traces). **D.** Light-adapted achromatic and dark-adapted chromatic (500 nm) horizontal sensitivity profiles in the patient compared with the normal range of sensitivity (gray bands = normal mean ± 2SD). Photoreceptor mediation is determined with the use of spectral sensitivity (500 nm - 650 nm) differences. When measurable, sensitivities were mediated by rods except at the normally cone-mediated foveal center (shown as a gap in the dark-adapted sensitivity profile). Hatched bars denote the location of the blind spot. N, nasal. T, Temporal.

Figure 1

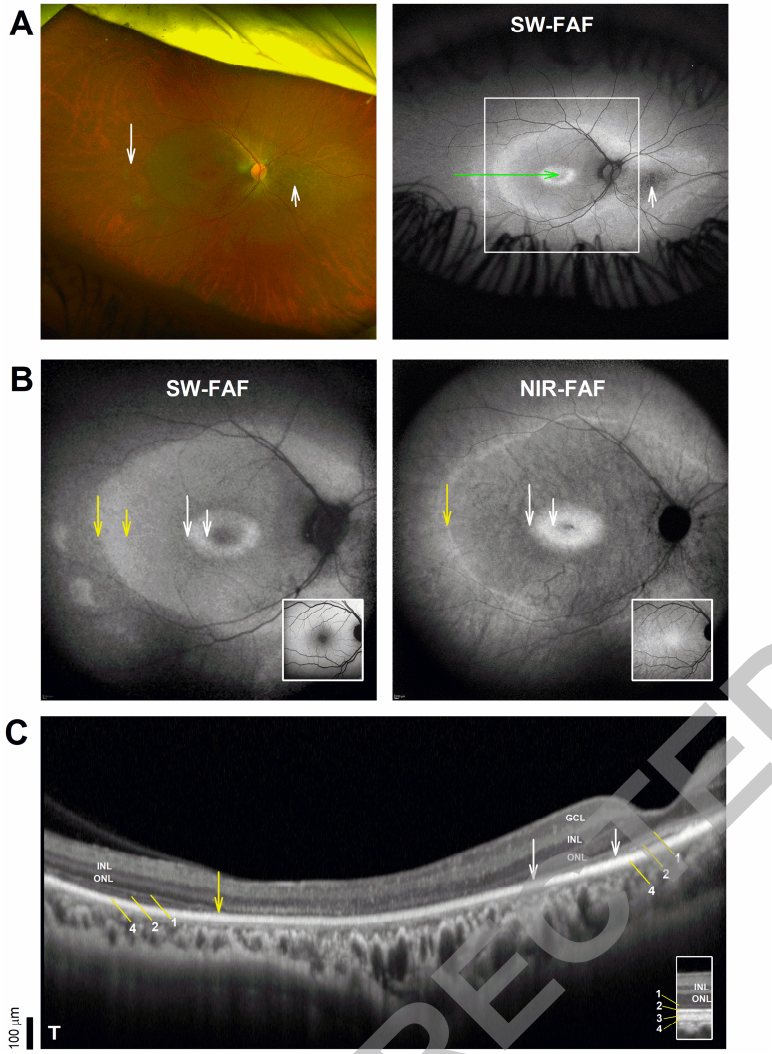

Figure 2